

A concrete heat accumulator for use in solar heating systems — a mathematical model and experimental verification

JACEK SACHARCZUK*
DAWID TALER

Cracow University of Technology, Faculty of Environmental Engineering,
Warszawska 24, 31-155 Kraków, Poland

Abstract The article presents a numerical model of the concrete heat accumulator for solar heating systems. Model uses control volume finite element method with an explicit solution method for time integration. The use of an explicit method is an essential advantage in the simulation of time-dependent changes in temperature of the air at the accumulator inlet. The study compares the results of numerical model calculations of the accumulator heating with experimental measurements and with computational fluid dynamics modeling. The comparison shows a good correlation between the results of calculation using the model and the results of measurements.

Keywords: Heat storage; Solar heating system; control volume finite element method

Nomenclature

a	–	thermal diffusivity, m^2/s
A	–	duct cross-section area, m^2
$A_{i,j,k}$	–	finite element surface area, m^2
c	–	specific heat of the accumulating material, $\text{J}/\text{kg K}$
c_p	–	specific heat of fluid, $\text{J}/\text{kg K}$
d_h	–	hydraulic diameter of air duct, m
L	–	length of air duct, m
Nu	–	Nusselt number
Pr	–	Prandtl number
\dot{q}	–	heat flux, W/m^2

*Corresponding Author. E-mail: sacharczuk@wp.pl

Q	–	heat accumulation, MJ
Re	–	Reynolds number
t	–	time, s
x, y, z	–	coordinates, m
T	–	temperature, °C
U	–	duct cross-section perimeter, m
w	–	air flow velocity, m/s

Greek symbols

α	–	heat transfer coefficient, W/m ² K
λ	–	thermal conductivity coefficient, W/mK
ρ	–	density, kg/m ³
ξ	–	Darcy friction factor

Subscripts

1, 2, 3	–	nodes numbers
a, b, c, O	–	midpoints and middle indexes
d	–	duct
f	–	fluid
m	–	model
p	–	measurement
w	–	wall surface

1 Introduction

Due to relatively short time of solar exposure during the day, solar systems have to co operate with heat storage systems. The most common and simplest system is based on accumulators storing heat in water. Although heat accumulation in water offers the greatest potential, the accumulators are limited by size. Therefore, research concentrates on alternative methods of heat storing based on specific heat of solids (stone, ceramics or heat-storing concrete) or on the phase change materials (concrete with the addition of paraffin wax for example). Although these materials have a relatively lower heat capacity, they offer quite a large potential for heat accumulation due to the possibility of incorporating them into structural components of the building or using the building unused space. The barriers to the application of such solutions are the lower storing temperature compared to water and the difficulties related to the transfer of heat from the collector loop to the heat storing material. The most common heat accumulation system storing heat in solids is a pebble bed unit heated with air. As these materials are relatively cheap, it is possible to build heat accumulators with a large capacity. The basic requirements for the pebble bed are good insulation, tightness and a small pressure drop of the air flow. Typically, a pebble

bed is laid in a box with concrete or wooden walls. The air heating the bed is usually supplied from air solar collectors. Air collectors are cheaper than liquid ones but less efficient. In order to ensure that the pressure drop in the bed does not exceed the acceptable level, the equivalent diameter of stones used in the bed has to be included in the range from 35 to 100 mm. The collector typical capacity is $0.15\text{--}0.3\text{ m}^3/\text{m}^2$.

The following assumptions are made in the modeling of such heat accumulators:

- air flow is one-dimensional,
- air and the bed material have constant thermal properties,
- heat conduction in the bed in the air flow direction is negligibly small,
- accumulator has a perfect insulation (no heat losses through the walls).

The process of pebble bed-based heat accumulation has been well-developed and described by means of lumped parameter models [1,2].

A concrete or ceramic heat accumulator in the form of a regular solid of an accumulating material with a system of internal air ducts can be an alternative to heat storing in a packed bed. Depending on the cycle phase, hot air is used either to heat the accumulator or to absorb the energy accumulated in it. Appropriate selection of the accumulator geometrical parameters, material thermal properties and heat transfer conditions in the ducts allows to spread the use of heat in time. Various materials can be used to make the accumulator, such as concrete, chamotte, ceramics, stone and even loose or slightly bound sand. It is appropriate to insulate the accumulator walls. In the case of accumulators with a duct structure, it is necessary to simulate the heat transfer process using the model with distributed parameters [3,4].

2 Numerical model of concrete accumulator

An attempt was made within the framework of conducted research to model the transient heat exchange in the accumulator with a duct structure. Such numerical modeling makes it possible to set time-dependent boundary conditions (the flow and temperature of the air heating and cooling the tank) corresponding to the solar system operation cycle. The aim of the modeling was to determine the optimum geometry of the accumulator cooperating with the solar system as well as to define its dynamic properties.

The accumulator with a duct structure is a concrete or ceramic structure made of blocks, e.g., hollow masonry units. Under the research scheme, a duct-structure accumulator was constructed of ready-made heat-storing elements used in fireplace systems [4]. Although the used modules have too large a cross-section of the air duct, which is adapted for the flue gas flow, owing to the module structure (key joint), the cross-section symmetry and favourable accumulation properties ($\rho = 2800 \text{ kg/m}^3$, $c = 940 \text{ J/kgK}$, $\lambda = 1.7 \text{ W/mK}$), they constitute a good material for modeling and experimental testing.

The assumption of the developed mathematical model of the transient heat transfer in the accumulator structure is that modeling the temperature distribution in repeatable modules determined in characteristic cross-sections is sufficient to obtain a correct description. If the cross-section of a module has one or more symmetry axes, modeling the temperature field in its repeatable part can be done. The concrete blocks used in the model experimental verification have a cross-section as shown in Fig. 1. It is characterized by four symmetry axes and for this reason a repeatable element corresponding to $1/8$ of the unit cross-section can be taken to model the temperature field. Two parallel series made of 8 blocks each were made in the experiment installation.

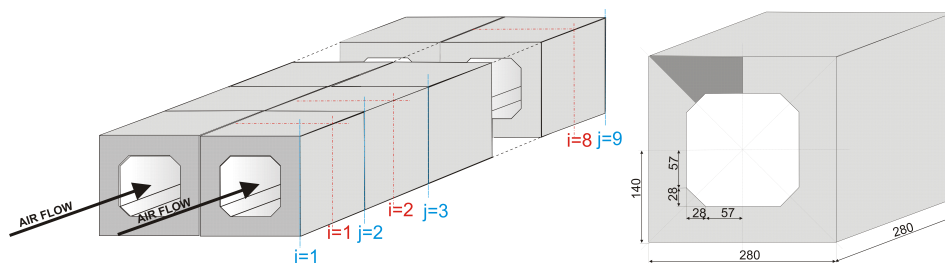


Figure 1: Diagram of the accumulator model structure and accumulation module geometry.

It is assumed that the temperature gradient in the material structure in the direction of axis z within individual modules is negligible. This makes it possible to analyse the temperature field in a two-dimensional system in the cross-sections determined by the planes of symmetry of individual accumulation modules ($i = 1, 2, \dots, 8$).

$$c(T)\rho(T)\frac{\partial T}{\partial t} = -\nabla \cdot \dot{q} = \frac{\partial}{\partial x} \left[\lambda(T) \frac{\partial T}{\partial x} \right] + \frac{\partial}{\partial y} \left[\lambda(T) \frac{\partial T}{\partial y} \right]. \quad (1)$$

However, the modelling requires taking account of the changes in temperature of the air flowing in the accumulator duct. Due to that, in order to perform the energy balance for the air flowing in the duct, planes are determined in the model ($j = 1, 2, \dots, 9$) corresponding respectively to the front and connection planes of the accumulator individual modules.

In order to solve the two-dimensional transient heat transfer problem in the planes of the accumulator cross-section, the control volume finite element method (CVFEM) is proposed [5]. The method allows temperature field modeling in a repeatable segment of the accumulator cross-section using a mesh of triangles based on a relatively small number of nodal points. In the CVFEM, the heat balance is made for the area surrounding each node, from the side of adjacent nodes. The partial area around the node is limited by the medians of the sides of a triangle coming from a given node. This ensures a symmetrical division of the triangle surfaces (the accumulating mass) among individual nodes.

In the case of a single triangular element 123 (Fig. 2), the energy balance in node 1 can be written as

$$\begin{aligned} c(T_1) \rho(T_1) \frac{A_{123}}{3} \frac{dT}{dt} = \\ = \lambda_x(T_o) \frac{y_c - y_a}{2A_{123}} [(y_2 - y_3) T_1 + (y_3 - y_1) T_2 + (y_1 - y_2) T_3] \\ + \lambda_y(T_o) \frac{x_c - x_a}{2A_{123}} [(x_2 - x_3) T_1 + (x_1 - x_3) T_2 + (x_2 - x_1) T_3], \quad (2) \end{aligned}$$

where a, b and c indicate the midpoints of respective sides.

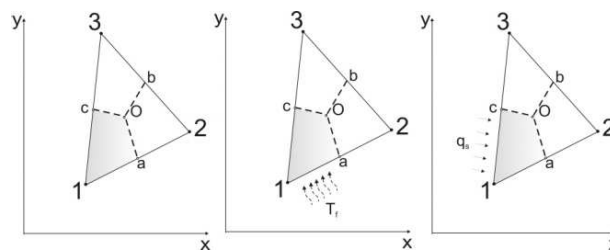


Figure 2: Single inner cell and boundary cells in the CVFEM.

For boundary conditions (e.g., convection occurring on side 1-2 and the inflow/outflow of heat q_s on side 1-3) the balance for the node 1 is

supplemented as follows:

$$\begin{aligned}
 c(T_1) \rho(T_1) \frac{A_{123}}{3} \frac{dT_1}{dt} = & \\
 \lambda_x(T_o) \frac{y_c - y_a}{2A_{123}} [(y_2 - y_3) T_1 + (y_3 - y_1) T_2 + (y_1 - y_2) T_3] & \\
 + \lambda_y(T_o) \frac{x_c - x_a}{2A_{123}} [(x_2 - x_3) T_1 + (x_1 - x_3) T_2 + (x_2 - x_1) T_3] & \\
 + \alpha \left[T_f - \left(\frac{3T_1}{4} + \frac{T_2}{4} \right) \right] s_{1a} + q_s s_{1c}, & \quad (3)
 \end{aligned}$$

where s_{1c} is the cell edge of 1-c length.

A division into control volumes formed around 16 nodal points is proposed for the analysed module constituting 1/8 of the unit cross-section (Fig. 3).

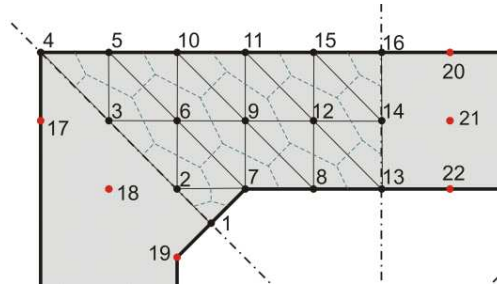


Figure 3: Division of the module of the accumulator cross-section into a finite element mesh.

In the segment under analysis, planes of symmetry can be determined for the temperature field 1-2-3-4 and 13-14-16. For these planes the temperature gradient in the normal direction equals zero. Similar conditions can be assumed for the external plane limiting the cross-section (nodes 4-5-10-11-15-16). Depending on its location in the accumulator structure, it is either the symmetry plane of two neighbouring segments or the plane adjacent to the insulation layer. For the boundaries of the area determined by nodes 1-2-3-4-5-10-11-15-16-14-13, the following boundary conditions can be assumed

$$\lambda \frac{\partial T}{\partial n} = 0. \quad (4)$$

The air temperatures in the accumulator duct $T_{f,i}$ in the Eq. [proszę podać!]

are assumed as arithmetic means for cross-sections j and $j + 1$ (Fig. 5).

$$T_{f,i} = \frac{T_{f,j} + T_{f,j+1}}{2}. \quad (5)$$

The air energy balance equation in the duct

$$\rho_f c_p \left(\frac{\partial T_f}{\partial t} + w \frac{\partial T_f}{\partial z} \right) = \frac{\dot{q}U}{A_d} = \frac{\alpha (\bar{T}_w - T_f) U}{A_d} \quad (6)$$

can be expressed in a finite-difference form

$$T_{f,j+1}^{k+1} = T_{f,j+1}^k + \Delta t \left(\frac{\alpha_j^k \left(\bar{T}_{w,i=j}^k - \frac{T_{f,i}^k + T_{f,i+1}^k}{2} \right) U}{A_d \rho_f c_p} - w \frac{T_{f,j+1}^k - T_{f,j}^k}{\Delta z} \right), \quad (7)$$

where \bar{T}_w is the mean internal surface temperature, Δt and Δz are the time and length steps, respectively.

If heat accumulation in the air flowing in the duct is neglected,

$$\frac{\partial T_f}{\partial t} = 0, \quad (8)$$

the temperature in the cross-section $j + 1$ is

$$T_{f,j+1}^k = \frac{T_{p,j}^k \left(1 - \frac{\Delta z \alpha_j^k U}{2 A_d \rho_f c_p w} \right) + \bar{T}_{w,i=j}^k \frac{\Delta z \alpha_j^k U}{A_d \rho_f c_p w}}{1 + \frac{\Delta z \alpha_j^k U}{2 A_d \rho_f c_p w}}. \quad (9)$$

The subscript j used in Eqs. (7) and (9) relates to subsequent cross-sections, whereas superscript k – to time interval. In cross-section $j = 1$ the air temperature is equal to the air temperature at the accumulator inlet. It can be seen that using the CVFEM, solving the problem of the transient heat transfer in the cross-section of the accumulator consisting of an isotropic material with constant thermal properties in the considered temperature range reduces to solving a system of ordinary differential equations in time, linear differential equations that can be solved using an explicit method. The number of equations for the entire accumulator is $16 \times (n - 1)$, where n is the number of modules making up the accumulator structure. The use of an explicit method is an essential advantage in the simulation of time-dependent processes occurring in the accumulator when the temperature

of the air at the accumulator inlet (what is inherent to the periodicity of obtaining the solar energy) [4].

The finite difference solution using an explicit method is stable if the Fourier and Courant-Friedrich-Lewy (CFL) conditions [6] are satisfied:

$$\frac{a\Delta t}{(\Delta x)^2} < \frac{1}{2} \frac{a\Delta t}{(\Delta y)^2} < \frac{1}{2} \frac{w\Delta t}{\Delta z} \leq 1, \quad (10)$$

where Δx and Δy are the mesh sizes in x and y coordinates, respectively.

The Gnielinski correlation [7] for $3 \times 10^3 \leq \text{Re} \leq 10^6$ is used to determine the heat transfer coefficient from air to the duct wall, taking account of the correction for the entry region:

$$\text{Nu} = \frac{(\xi/8)(\text{Re} - 1000)\text{Pr}}{1 + 12.7(\xi/8)^{1/2}(\text{Pr}^{2/3} - 1)} \left[1 + \left(\frac{d_h}{L} \right)^{2/3} \right], \quad (11)$$

where Pr is the Prandtl number, d_h and L is hydraulic diameter and length and the Darcy-Weisbach friction coefficient is given by

$$\xi = [0.79 \ln(\text{Re}) - 1.64]^{-2}. \quad (12)$$

The results of comparative calculations indicate that the Gnielinski correlation gives a better fit than the commonly used Dittus-Boelter formula in the form

$$\text{Nu} = 0.023\text{Re}^{0.8}\text{Pr}^n, \quad (13)$$

where n is equal to 0.4 for heating and 0.3 for cooling.

The problem was solved using a computational program written in Fortran. The program makes it possible to simulate the transient heat transfer process at set parameters of the heating air and to combine the system with water-air exchanger, which is fed from a solar system or from a tank with an external source of heat.

3 Experimental study and CFD modeling

The model was verified by comparing the numerical calculation results to the results of measurements made on the experimental facility during the accumulator heat-up.

For the purpose of experimental verification, an installation composed of a concrete heat accumulator and an air circulation system heated by

a plate-fin-and-tube heat exchanger was built (Figs. 4 and 5). The heat exchanger was fed with hot water from a 0.2 m³ tank heated by a gas boiler with temperature controlled by means of a boiler controller and additionally by an electric heater. The target of the system design is to cooperate with a solar collector. The system makes it possible to stabilise the temperature in the feeding tank but in trial measurements the phase of water heating in the tank with time dependent water temperature was also studied.

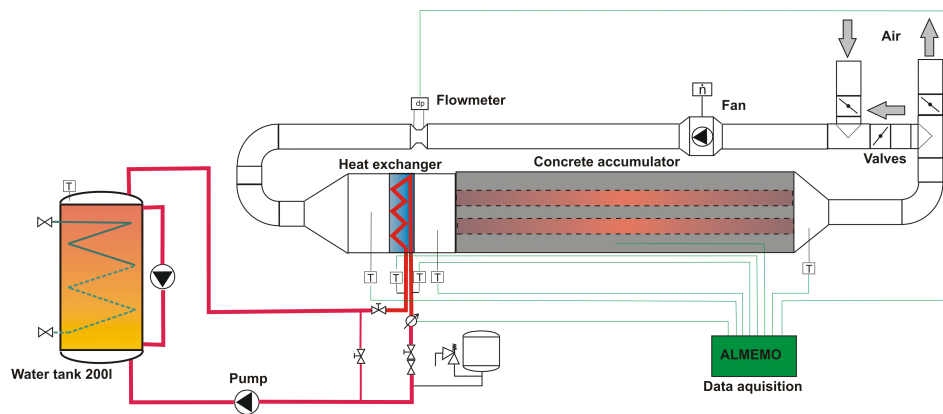


Figure 4: Diagram of the stand.



Figure 5: Test stand (Cracow Institute of Thermal Engineering and Air Protection, Cracow UT).

The heating time was 12 h. During the measurements, the flow rate and temperature of water were recorded at the air heater inlet and outlet. Also the flow rate and temperature of air – before and after the heater and before and after the accumulator, were measured using the data acquisition system. The purpose of the measurements on the heating water side (as more accurate ones) was to check the agreement of the heat balance on the air side and to verify the measurements of temperature of the air flowing into the accumulator duct. Heat transfer rate differences for the air heater did not exceed 5%, which should be deemed as satisfactory, considering the precision of applied measuring devices (flow meter with a vortex transducer and type K thermocouples on the water side, and a hot-wire anemometer and class A Pt100 resistance thermometers on the air side).

The next verification stage was to compare the heat flow rate transferred from the air to the accumulator with the heat flow rate accumulated by concrete accumulator. Four twelve-hour tests of the accumulator heating were used for the analysis. The tests were performed under the conditions of a gradual rise in temperature in the water tank and at a more or less stabilised water temperature in the tank. The air flow rate in the accumulator duct stayed at the level of 1.3 to 2.7 m/s (the Reynolds number ranging from 14800 to 30000).

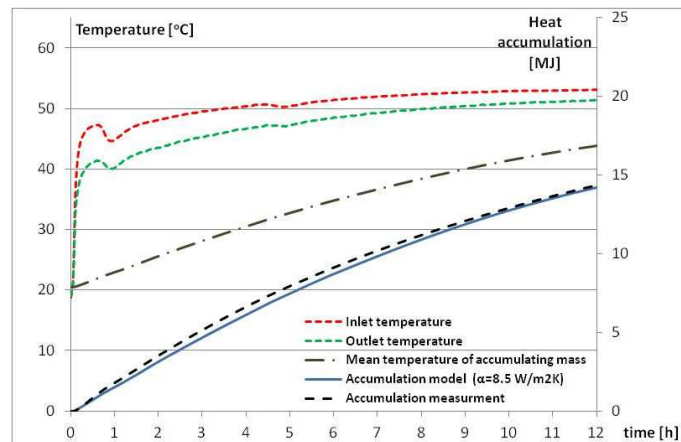
Comparing the balance of energy accumulated in the storing material (calculated based on the presented numerical model) to the balance of heat transferred to the accumulator by the air flowing in the duct (determined based on measurements of the air flow rate and temperatures at the accumulator inlet and outlet), a good agreement between the results of measurements and calculations was obtained.

Table 1 summarises results of measurements and calculations for four different cases of the accumulator heating. Figures 6-9 present a comparison of the calculation results with the measurement data in a form of time-dependent curves illustrating accumulated energy in the storing material (according to the model), thermal energy transferred by the air flowing in the ducts (measurement data) and temperatures measured at the accumulator inlet and outlet.

In further analyses, the simulation results obtained with the developed mathematical model were compared to the simulation performed using the commercial computational fluid dynamics (CFD) software (ANSYS Fluent v. R14.5), [8]. The simulation was made assuming a constant air flow rate and air temperature at the accumulator inlet +60 °C (Fig.12). The

Table 1: Results of heat accumulation calculations obtained by using the proposed mathematical model (Q_m) compared to measurements (Q_p), $\delta Q = (Q_m - Q_p)/Q_m$.

Time [h]	1	2	3	4	6	8	10	12
Test 1: $\alpha_{mean} = 8.5 \text{ W}/(\text{m}^2\text{K})$								
Q_m [MJ]	1.54	3.15	4.68	6.12	8.72	10.90	12.75	14.21
Q_p [MJ]	1.81	3.54	5.16	6.64	9.13	11.19	12.92	14.37
δQ [%]	-17.7	-12.3	-10.3	-8.5	-4.8	-2.7	-1.3	-1.1
Test 2: $\alpha_{mean} = 10.6 \text{ W}/(\text{m}^2\text{K})$								
Q_m [MJ]	1.91	3.68	5.43	6.97	9.58	11.84	13.72	15.19
Q_p [MJ]	1.95	3.72	5.35	6.78	9.18	11.31	13.06	14.52
δQ [%]	-2.3	-1.2	1.4	2.8	4.1	4.5	4.8	4.4
Test 3: $\alpha_{mean} = 7.6 \text{ W}/(\text{m}^2\text{K})$								
Q_m [MJ]	0.56	1.67	2.97	4.35	7.05	9.51	11.62	13.32
Q_p [MJ]	0.47	1.62	3.04	4.52	7.31	9.71	11.75	13.43
δQ [%]	15.4	3.3	-2.2	-3.7	-3.7	-2.1	-1.1	-0.8
Test 4: $\alpha_{mean} = 12.1 \text{ W}/(\text{m}^2\text{K})$								
Q_m [MJ]	0.89	2.21	3.79	5.42	8.47	11.23	13.37	15.03
Q_p [MJ]	0.83	2.11	3.66	5.24	8.17	10.85	13.03	14.87
δQ [%]	6.90	4.50	3.70	3.30	3.60	3.40	2.50	1.10

Figure 6: Heating process curves: $\alpha_{mean} = 8.5 \text{ W}/(\text{m}^2\text{K})$, feed temperature stable 45–53 °C.

developed numerical model assumed a constant value of the heat transfer coefficient in the analysed duct section (2.24 m). The value, calculated from the Gnielinski correlation taking account of the run-up section, was $10.1 \text{ W}/(\text{m}^2/\text{K})$, whereas the CFD simulation showed higher values of coefficient α ($13.5 \text{ W}/(\text{m}^2/\text{K})$ on average) and considerable variations of the coef-

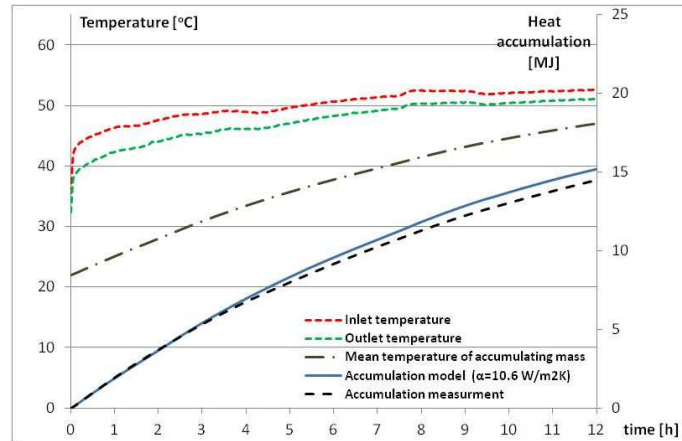


Figure 7: Heating process curves: $\alpha_{mean} = 10.6 \text{ W}/(\text{m}^2\text{K})$, feed temperature stable 45–53 °C.

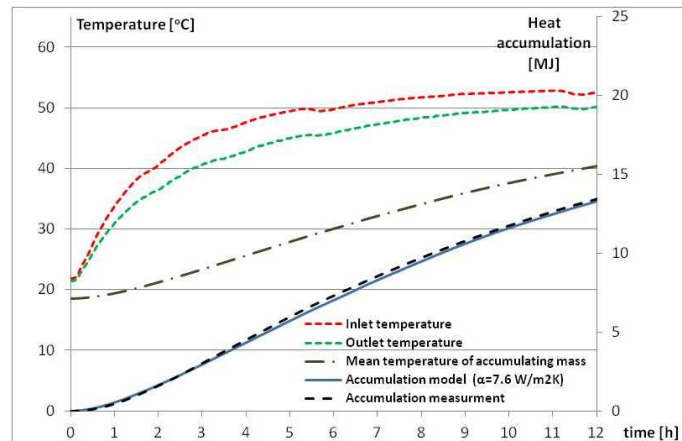


Figure 8: Heating process curves: $\alpha_{mean} = 7.6 \text{ W}/(\text{m}^2\text{K})$, feed temperature rising 20–53 °C.

ficient along the duct length, with a local rise in its value to $14.29 \text{ W}/(\text{m}^2\text{K})$ in the initial section. In consequence, the accumulating mass temperature gradient found in the structure along the duct length was much higher than the gradient obtained in the simulation made with the in-house model. In the CFD simulation, the accumulating mass temperatures after 8 hours of heating differed by 7.65 K (from 42.03 °C in the duct inlet cross-section to 49.68 °C in the outlet cross-section). The simulation performed using

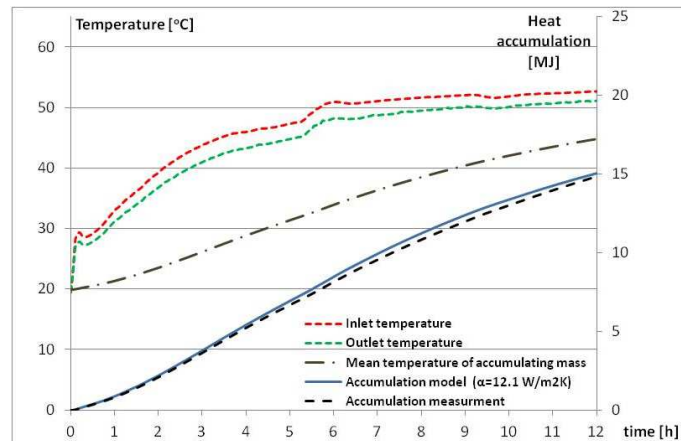


Figure 9: Heating process curves: $\alpha_{mean} = 12.1 \text{ W}/(\text{m}^2\text{K})$, feed temperature rising 20–53 °C.

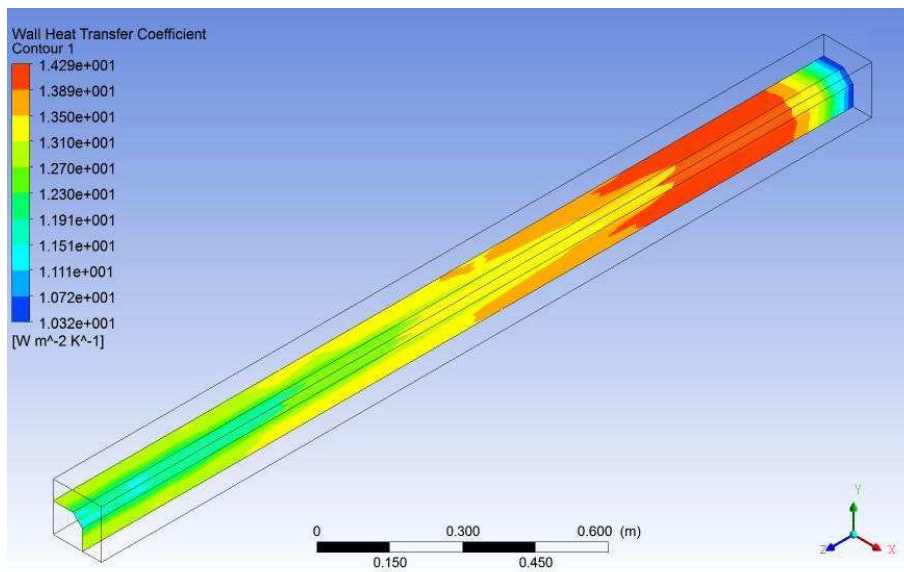


Figure 10: Heat transfer coefficient distribution after 8 h of heating in the CFD simulation.

the in-house model showed an only 2.79 K difference (from 46.03 °C in the duct inlet cross-section to 48.82 °C in the outlet cross-section). Designing the test stand, no comparative measurements of the accumulating mass temperatures in different cross-sections of the duct were anticipated. For

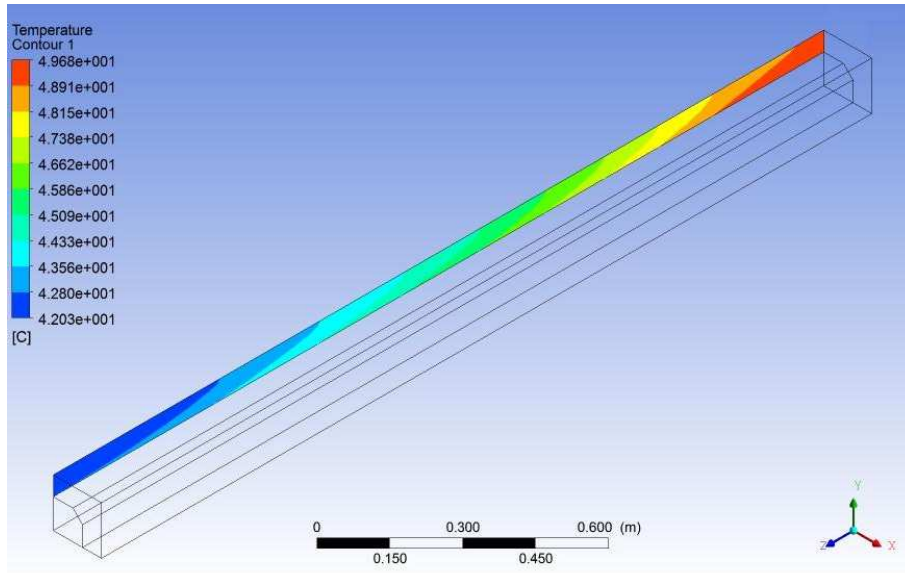


Figure 11: Temperature distribution in the longitudinal section of walls after 8 h of heating in the CFD simulation.

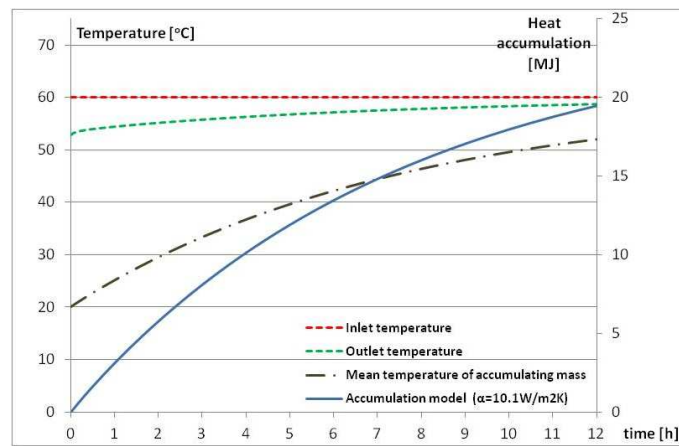


Figure 12: Heating process curves: $\alpha_{mean} = 10.1 \text{ W/m}^2\text{K}$, constant feed temperature – 60 °C according to the model simulation.

this reason, it was impossible to verify this particular effect experimentally. However, analysing measured changes in the temperature of air between the inlet and outlet cross-sections, it can be said that they correspond more

closely to the temperature distribution obtained using the in-house model (after 8 h of heating, the air temperatures at the inlet and outlet differed only by 3.2 K).

4 Conclusions

The mathematical model of the heat accumulator developed in the paper can be used to calculate with a high accuracy the heat accumulated in the concrete duct structures. The calculation method has been verified by experimental results. The CVFEM method allows to solve transient heat conduction problems based on a small number of elements, compared to classic FEM. The method is not only much faster than commercial CFD software simulations but the results are in a better agreement with the experimental data. Solution to the problem by explicit method allows modeling the complex shapes of solid heat storing elements and variable boundary conditions using simple Fortran software.

Received 18 June 2014

References

- [1] DUFFIE J., BECKMANN W.: *Solar Engineering of Thermal Processes*. Wiley Interscience, New York 1991.
- [2] DOMAŃSKI R.: *Thermal Energy Storing*. PWN, Warsaw 1990 (in Polish).
- [3] TALER D., CISEK P.: *Modeling of cooling of ceramic heat accumulator*. Arch. Thermodyn. **34**(2013), 4, 161–173.
- [4] SACHARCZUK J., TALER D.: *Using concrete or ceramic units to store heat obtained in a solar installation*. Rynek Energii **4**(2013), 107, 37–42 (in Polish).
- [5] TALER J., DUDA P.: *Solving Direct and Inverse Heat Conduction Problems*. WNT, Warsaw 2003 (in Polish).
- [6] COURANT R., FRIEDRICHS K., LEWY H.: *On the partial difference equations of mathematical physics*. IBM J. Res. Development **2**(1967), 11, 215–234.
- [7] INCROPERA F.P., DEWITT D.P.: *Fundamentals of Heat and Mass Transfer*, 3rd Ed. Wiley, New York 1990.
- [8] ANSYS-Fluent User's Guide. ANSYS, 2011.